Physics Letters A 380 (2016) 3313–3318

Contents lists available at ScienceDirect

Physics Letters A

www.elsevier.com/locate/pla

Discovery of superparamagnetism in sub-millimeter-sized magnetite porous single crystals

Ji Ma, Kezheng Chen *

Lab of Functional and Biomedical Nanomaterials, College of Materials Science and Engineering, Qingdao University of Science and Technology, Qingdao 266042, China

ARTICLE INFO

Article history:
Received 18 July 2016
Received in revised form 27 July 2016
Accepted 30 July 2016
Available online 4 August 2016
Communicated by M. Wu

Keywords:
Magnetite
Superparamagnetism
Single crystal
Porous
Molecular field theory

ABSTRACT

In this work, sub-millimeter-sized magnetite porous single crystals were found to exhibit unique superparamagnetism rather than the known ferrimagnetism. This superparamagnetism was intimately related to the hydrothermal formation process, during which high lattice stress of ca. 6 GPa and large lattice strain of ca. -1.21×10^{-2} would change the exchange constants of α, β, and ν to concurrently meet criterions of (i) $\nu_1 = \nu_2 = \beta$, (ii) $\alpha_1 = \alpha_2 = \alpha$, and (iii) $\alpha\beta = 1$. These criterions, deduced from the molecular-field theory, were proposed to be the general transition conditions for any ferrimagnetic material exhibiting superparamagnetism when their size was beyond their superparamagnetic size limit.

1. Introduction

Recently, there is an increasing interest in the study of superparamagnetic (SPM) single crystals exposing specific facets owing to their highly reactive surfaces and outstanding magnetic performance [1–4]. Among these SPM materials, iron oxides have drawn much attention because of their biocompatible and stable features [5–7]. Unfortunately, two kinds of dilemmas linger around their current and foreseen applications, including catalytic, magnetic, electronic, and biomedical types. On the one hand, the relatively low specific surface area of single crystals crucially limits their exposed reactive surfaces, especially when their size exceeds micrometer scale [8]. On the other hand, the size of single crystals is generally on the order of 10 nm to maintain their SPM characteristics. In this case, these nanocrystals possess low saturation magnetization. As a result, it is hard to effectively separate them from solution or control their movement by using moderate magnetic fields. This greatly limits their usage in some practical applications such as separation and targeted delivery [7]. Increasing the crystal size synchronously increases their saturation magnetization, but it can also induce the SPM-ferromagnetic (FM) transition, so that these crystals are no longer dispersible in solution. To address these formidable challenges, a new strategy of developing porous single crystals (PSCs) [8] not only offers high specific surface area while exposing enormous highly reactive surfaces and facilitates fast charge transfer across the crystal framework, but also has the advantage of increasing the SPM magnetization in a controllable manner on condition that the SPM characteristics still remain where possible.

Herein, magnetite (Fe_3O_4) PSCs were fabricated by a facile hydrothermal treatment. Although these quasi-octahedral crystals were hundreds of micrometers in edge length, they exhibited unique SPM characteristics rather than FM behaviors in this size range. This is, to the best of our knowledge, the first finding of SPM performance in sub-millimeter-sized single crystals. It is anticipated that this finding will shed new light on the development of SPM bulk materials.

2. Experimental

2.1. Synthesis of magnetite PSCs

All chemicals were analytical grade and used as received without further purification. Typically, 20 mL of $K_3[Fe(CN)_6]$ aqueous solution (0.5 mol/L) and 20 mL of ethylenediamine were mixed together under vigorous stirring for 10 min. The resultant solution was transferred into Teflon-lined stainless-steel autoclaves with a capacity of 100 mL for hydrothermal treatment at 220 °C for 24 h. The as-obtained precipitate was repeatedly washed with deionized water and ethanol, and finally dried at 70 °C for 4 h. As a comparison, a part of the Fe_3O_4 PSCs was calcined at 800 °C for 2 h in

* Corresponding author. Fax: +86 532 84022509.
E-mail address: kchen@qust.edu.cn (K. Chen).

http://dx.doi.org/10.1016/j.physleta.2016.07.065
0375-9601/

the atmosphere of nitrogen, and underwent furnace cooling subsequently.

2.2. Characterization

XRD patterns were recorded on a powder X-ray diffractometer (Rigaku D/max-rA) equipped with a rotating anode and a Cu-$K_{\alpha 1}$ radiation source ($\lambda = 1.5406$ Å) at a step width of 0.02°. Scanning electron microscope (SEM) images were collected on a field-emission scanning electron microscope (JEOL JSM-6700F). Transmission electron microscopy (TEM) was performed on the JEOL 2010 TEM with an operating voltage of 200 kV. The high-resolution electron microscopy (HRTEM) experiments were conducted using a Field Emission Gun (FEG) JEOL 2010F microscope with a point resolution of 0.19 nm. The HRTEM sample was prepared in the following procedure. Firstly, the as-synthesized product was mixed with the polymer resin and solidificated at 80 °C in vacuum oven overnight. Afterwards, the cured resin was cut into thin slices in 60 nm-thickness using ultramicrotome (PowerTomeXL) for HRTEM observation. The magnetic measurements of powder samples were conducted on superconducting quantum interference device (SQUID) magnetometry (MPMS-5XL, Quantum Design).

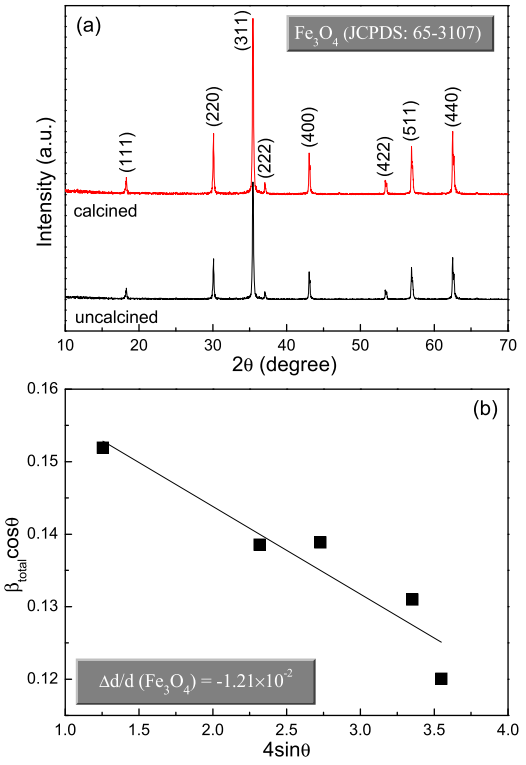

Fig. 1. (a) XRD patterns of the as-synthesized Fe_3O_4 PSCs before and after calcination. (b) Linear fitting of XRD peaks of uncalcined Fe_3O_4 PSCs using Williamson–Hall relationship.

3. Results and discussion

The XRD patterns of Fe_3O_4 PSCs before and after calcination in Fig. 1(a) reveal intense and sharp peaks that can be unambiguously indexed to the cubic structure of Fe_3O_4 according to the Joint Committee on Powder Diffraction Standards (JCPDS) card No. 65-3107. The lattice constant of Fe_3O_4 PSCs is determined to be 8.385 Å, which is a bit smaller than that of the calcined Fe_3O_4 PSCs (ca. 8.392 Å). Then, the lattice strain was calculated according to the Williamson–Hall relationship [9], given by

$$\beta_{total} = \frac{0.9\lambda}{t\cos\theta} + \frac{4(\Delta d)\sin\theta}{d\cos\theta} \tag{1}$$

where β_{total} is the full-width at half-maximum (FWHM) of the XRD peak, λ is the incident X-ray wave length, θ is the diffraction angle, t is the crystal size, and Δd is the difference of the d spacing corresponding to a typical peak. A plot of $\beta_{total}\cos\theta$ against $4\sin\theta$ yields the crystal size t of ca. 8 nm from the intercept [Fig. 1(b)], indicating these sub-millimeter-sized Fe_3O_4 single crystals are formed by the oriented attachment of finite-sized particles. In this scenario, large lattice strain (or stress) may be present in the product. Further, the lattice strain ($\Delta d/d$) of the Fe_3O_4 product can be directly determined from the slope in Fig. 1(b), which gives the value of -1.21×10^{-2}. This strain value is two orders of magnitude higher than those of other Fe_3O_4 structures [10]. Such large lattice strain (or stress) will greatly influence the strength of superexchange interaction among Fe–O–Fe ions [11].

Fig. 2(a) shows a typical quasi-octahedral morphology of the Fe_3O_4 product with an average edge length of 0.2 mm. These huge

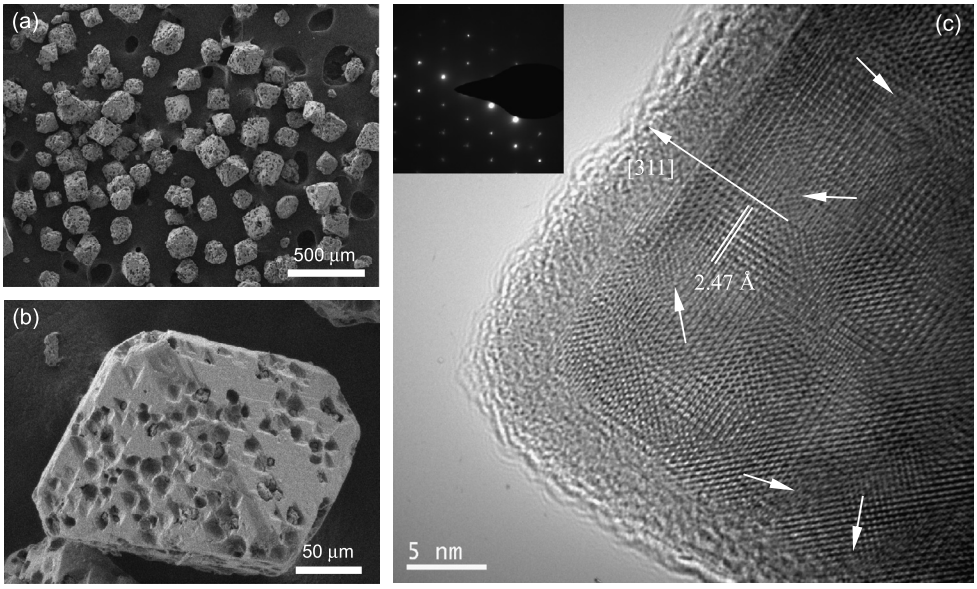

Fig. 2. SEM images of the as-synthesized Fe_3O_4 product with (a) low- and (b) high-magnification. (c) HRTEM image of the product with arrows indicating typical lattice defects. The surface amorphous layer is attributed to the coated resin yielded from the HRTEM slice procedure. The SAED pattern is shown as an inset.